



LAWRENCE
LIVERMORE
NATIONAL
LABORATORY

Simulations of NSTX with a Liquid Lithium Divertor Module

D. P. Stotler, R. Maingi, L. Zakharov, H. W. Kugel,
A. Yu. Pigarov, T. D. Rognlien, V. A.
Soukhanovskii

August 31, 2009

Contributions to Plasma Physics

Disclaimer

This document was prepared as an account of work sponsored by an agency of the United States government. Neither the United States government nor Lawrence Livermore National Security, LLC, nor any of their employees makes any warranty, expressed or implied, or assumes any legal liability or responsibility for the accuracy, completeness, or usefulness of any information, apparatus, product, or process disclosed, or represents that its use would not infringe privately owned rights. Reference herein to any specific commercial product, process, or service by trade name, trademark, manufacturer, or otherwise does not necessarily constitute or imply its endorsement, recommendation, or favoring by the United States government or Lawrence Livermore National Security, LLC. The views and opinions of authors expressed herein do not necessarily state or reflect those of the United States government or Lawrence Livermore National Security, LLC, and shall not be used for advertising or product endorsement purposes.

Simulations of NSTX with a Liquid Lithium Divertor Module

D. P. Stotler^{*1}, R. Maingi², L. E. Zakharov¹, H. W. Kugel¹, A. Yu. Pigarov³, T. D. Rognlien⁴, and V. A. Soukhanovskii⁴

¹ Princeton Plasma Physics Laboratory, Princeton University, P.O. Box 451, Princeton, NJ 08543-0451, USA

² Oak Ridge National Laboratory, Oak Ridge, TN 37831, USA

³ University of California at San Diego, San Diego, CA, USA

⁴ Lawrence Livermore National Laboratory, Livermore, CA 94551, USA

Received 15 November 2003, revised 30 November 2003, accepted 2 December 2003

Published online 3 December 2003

Key words List, of, comma, separated, keywords.

PACS 52.55.Fa, 52.65.-y, 52.40.Hf, 61.25.Mv

A program to develop self-consistent simulations of the behavior of lithium in the Liquid Lithium Divertor (LLD) module to be installed in NSTX is described. In this initial stage of the program, the UEDGE edge plasma transport code is used to simulate an existing NSTX shot, with UEDGE's transport coefficients set using midplane and divertor diagnostic data. The LLD is incorporated into the simulations as a reduction in the recycling coefficient over the outer divertor. Heat transfer calculations performed using the resulting heat flux profiles provide preliminary estimates on operating limits for the LLD as well as input data for subsequent steps in the LLD modeling effort.

Copyright line will be provided by the publisher

1 Introduction

The National Spherical Torus eXperiment (NSTX, $R = 0.85$ m, $a < 0.67$ m, $R/a > 1.27$) [1] has been investigating the use of lithium as a surface coating material to improve plasma performance and to provide better control of the core plasma density. The latter will permit prescribed density scans in long-pulse H-modes. Operation at low plasma densities also increases the fraction of plasma current driven by neutral beams, resulting in longer discharges. The lithium program has proceeded in stages, beginning with lithium pellet injection in 2005. In 2006, an evaporative lithium system (LiThium EvaporatoR, or LiTER) was installed to coat the graphite tiles that serve as the primary plasma facing material in NSTX [2]. The 2006 – 2007 experiments resulted in 50% reductions in L-mode density and 15% reductions in H-mode [2]. During the 2008 and 2009 campaigns, two evaporators were used, resulting in improved energy confinement times ($\tau_E > 100$ ms), longer pulse lengths (1.8 s) [3], and reduced Edge Localized Mode activity [4]. The core density still increases monotonically during these discharges, although some or all of this increase is attributed to sputtered carbon and other impurities [3]. To provide greater control of the core deuteron content and to continue investigating these other performance improvements, NSTX is pursuing the next step in this progression of lithium usage, the Liquid Lithium Divertor (LLD), which will place a thicker, toroidally continuous liquid lithium surface in contact with the plasma.

The LLD is a joint collaboration between Sandia National Laboratory, University of California at San Diego, and the NSTX project. The basic concept is of a toroidally extended lithium containing tray that

* Corresponding author: e-mail: dstotler@pppl.gov, Phone: +1 609 243 2063, Fax: +1 609 243 2662

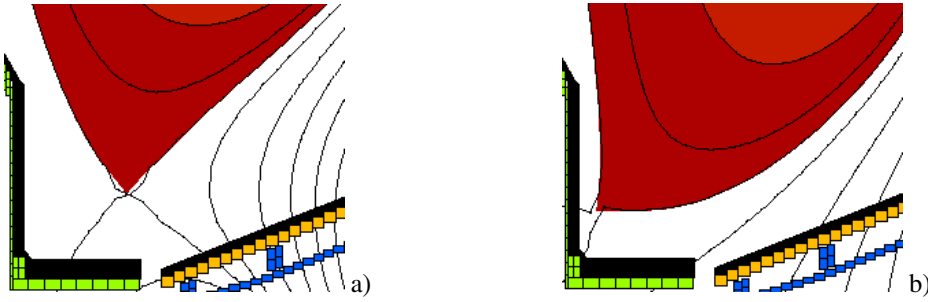


Fig. 1 The outer strike point of low triangularity (0.45) discharges **a** hits the LLD directly; with high triangularity (0.7) **b**, pumping will be farther out in the SOL.

will serve as a target for the outer strike point or divertor. Ideally, the radial location and width of the tray would be chosen so as to obtain the greatest degree of density reduction for both low and high triangularity discharges (Fig. 1). However, practical and programmatic considerations also enter; these favor placing the tray on the outer divertor target plate just outside the co-axial helicity injection gap. Simple particle balance calculations suggest that in this location the core density will be reduced by about 50% for low triangularity (strike point directly on the LLD) and by about 25% with high triangularity. One of the objectives of the modeling effort associated with this paper is to put these estimates on a firmer footing.

We describe here modeling of the scrape-off layer (SOL) plasma conditions under LLD operation and the resulting temporal evolution of the temperature of the lithium surface. Section 2 discusses modeling of an existing NSTX discharge with the 2-D edge plasma transport code UEDGE [5]. With this as a baseline, we then (Sec. 3) vary the outer divertor recycling coefficient, representing the effect of the LLD on the SOL plasma. The thermal response of the LLD to these plasma conditions is estimated with a 3-D heat transfer calculation in Sec. 4. Subsequent steps in this LLD modeling effort are described in Sec. 5.

2 Calibration of UEDGE Transport Model

The UEDGE-2D edge plasma transport code [5] solves fluid equations for ion density, electron and ion temperature, ion parallel flow velocity, and electrostatic potential. Transport along field lines is classical with flux limits incorporated to replicate important kinetic effects. Anomalous transport across field lines simulates the effects of plasma turbulence, including the intermittent transport associated with “blobs” [6]. A Navier-Stokes fluid model describes the behavior of neutral deuterium. Because we will subsequently impose dramatic changes to the boundary conditions (the pumping provided by the LLD), we ignore subtler effects such as those associated with the multiple charge state carbon model and classical drifts.

We use an existing NSTX discharge to establish the input parameters to UEDGE. First, we derive a computational mesh from the equilibrium of a low triangularity, single null discharge similar to that shown in Fig. 1a (shot 128339 at 0.35 s; toroidal magnetic field = 0.5 T, plasma current = 1 MA). Not only is the strike point for this discharge located within the planned LLD location, so is the entire outer divertor target of the computational mesh. Hence, we will simulate the pumping effect of the LLD as a uniform reduction in recycling there. Since initial operation with the LLD will be conservative, the time slice chosen for these initial simulations has only 1 MW of neutral beam power.

This computational mesh spans normalized flux values $\psi_n = \psi/\psi_{sep} = 0.85 - 1.07$. The electron density and temperature at the core boundary are obtained from the Thomson scattering diagnostic: $4.3 \times 10^{19} \text{ m}^{-3}$ and 130 eV, respectively. Ion temperature data from charge-exchange spectroscopy do not extend this far in radius; instead we note that $T_i \sim T_e - 15 \text{ eV}$ at slightly smaller radii and set the ion temperature boundary condition to 115 eV.

We specify on input to UEDGE the particle diffusivity D , electron thermal diffusivity χ_e , and anomalous radial convective velocity v ($v > 0$ represents radially outward flow) with values given at the core boundary, separatrix and outer wall (D_c , D_s , and D_w , etc.). The values in between are computed via linear interpolation on the radial mesh index; all coefficients are constant on a flux surface. The ion thermal diffusivity $\chi_i = \chi_e$, and the cross-field diffusivity of parallel momentum is set to $2/3\chi_e$. Our approach is thus intended to be more elaborate than that in [7], but less so than that described in [6], in which a 2-D characterization of transport was developed specifically to investigate the connection between poloidal asymmetries in the radial transport coefficients and high speed SOL flows.

Second, we adjust the D , χ_e , and v values to match the midplane Thomson scattering n_e and T_e profiles, as well as the power flowing in from the core. The latter is estimated to be in the range of 1.7 – 1.8 MW (1 MW NBI, \simeq 1 MW OH, \sim 15% beam ion loss, and $<$ 0.1 MW of core radiation). For particle balance, we lump all external fueling into the core particle source and require its magnitude to be consistent with the sum of center stack gas puff (about 400 A) and NBI fueling (18 A).

Since we have no experimental data with which to constrain transport within the private flux region (PFR) and since the plasma parameters elsewhere are relatively insensitive to it, we treat the PFR diffusivity as a free parameter that can be adjusted as needed to yield PFR densities $> 10^{17} \text{ m}^{-3}$ to maintain UEDGE convergence.

The simulated density profile obtained with transport coefficients $D_c = 0.04$, $D_s = D_w = 0.1 \text{ m}^2/\text{s}$, $v_c \equiv 0$, $v_s = 25$, $v_w = 30 \text{ m/s}$ is shown in Fig. 2. Note the very different shape and separatrix density obtained with a nominal, constant $D = 0.5 \text{ m}^2/\text{s}$ and $v = 0$. The thermal diffusivities are $\chi_{e,c} = 1.5$, $\chi_{e,s} = 25$, and $\chi_{e,w} = 35 \text{ m}^2/\text{s}$. The Thomson scattering profile shows a separatrix temperature of only 10 eV. However, this is likely the result of a slight inaccuracy in separatrix location since power balance considerations and a simple 2-point model indicate separatrix temperatures in the 30 – 40 eV range. Hence, our baseline profiles sit well above the experimental ones in the SOL. The profile obtained with a constant $\chi_e = 1 \text{ m}^2/\text{s}$ differs only slightly in the outer SOL, but corresponds to an input power of just 0.75 MW.

The total power flowing in from the core boundary in our baseline simulation is $P_e = 0.98 \text{ MW}$ and $P_i = 0.82 \text{ MW}$, for a total of 1.8 MW, consistent with experimental power balance. The D^+ current flowing into the problem from the core boundary is 440 A, and a 142 A current of D atoms is flowing through this boundary in the other direction; again this is compatible with the experimental particle balance.

We also verify that the simulation reasonably reproduces the available data along the outer divertor target where the LLD will be situated. The heat flux is determined experimentally by analysis of infrared emission from the graphite divertor tiles [8]. Profiles from two time slices around the time of interest (0.35 s) are plotted in Fig. 3a as a function of major radius along the divertor floor. We also compare with the D_α emission seen by divertor camera [9]. Since D_α calibration data for shot 128339 will be available only after the end of the present NSTX run campaign, we instead utilize D_α data from shot 125065 at 0.4 s, which has the same magnetic configuration, core density and input power as 128339 at 0.35 s.

The simulated profiles are affected by the amount of pumping (or absorption) of deuterium ions (“recycling” \mathcal{R}) and atoms (“albedo” \mathcal{A}) by graphite surfaces at various locations around the vacuum vessel. In both, cases a value of unity implies that the surface does no pumping / absorption. Following [11], we assume a nominal amount of pumping by unsaturated graphite surfaces with recycling coefficients and albedos that are equal at the outer wall $\mathcal{R}_w = \mathcal{A}_w = 0.95$, nearly unity at the inner divertor $\mathcal{R}_{id} = 0.99$, $\mathcal{A}_{id} = 1$, and slightly lower on the outer divertor $\mathcal{R}_{od} = \mathcal{A}_{od} = 0.98$. The resulting divertor profiles are compared with the experimental data and a corresponding simulation with unit recycling in Fig. 3. The two simulated heat flux profiles are similar, but some amount of pumping is essential to bring the D_α emission rate within a factor of two of the observations. Note that neither simulation agrees with the D_α emission in the inner divertor. Improving agreement there requires an approach along the lines described in Ref. [11] and probably physics not included there. A more sophisticated Monte Carlo neutral transport simulation (using DEGAS 2 [10]) performed with the baseline plasma yields essentially the same

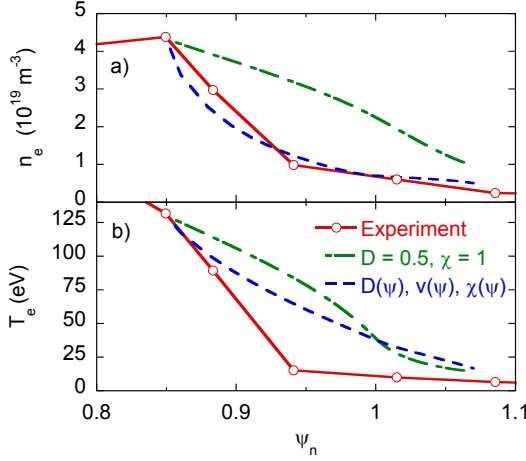


Fig. 2 Comparison of experimental midplane n_e **a** and T_e **b** profiles with a constant coefficient ($D = 0.5$ and $\chi_e = 1 \text{ m}^2/\text{s}$) UEDGE simulation and with our baseline simulation having radially varying transport coefficients.

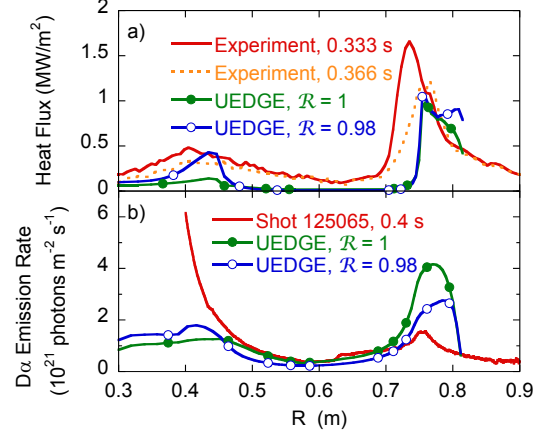


Fig. 3 **a** Comparison of the outer divertor experimental heat flux with the baseline UEDGE simulation ($\mathcal{R} = 0.98$) and a variant with unit recycling. **b** Comparison of the same two simulations with divertor D_α emission from the similar shot 125065.

D_α profile, demonstrating that UEDGE’s neutral calculation is reasonable. Henceforth, we will only be varying \mathcal{R}_{od} and \mathcal{A}_{od} ; for brevity we will refer to them as the “recycling coefficient” $\mathcal{R} = \mathcal{R}_{od} = \mathcal{A}_{od}$.

3 Scan of Recycling Coefficient

The absolute minimum value of recycling obtainable with a clean lithium target is set by the particle reflection coefficient and is expected to be in the 0.1 – 0.3 range. However, the actual values obtained in the experiment will likely be higher due to variations in coating thickness and surface contamination [12]. Since we cannot predict these factors, we perform a scan over the recycling coefficient.

We first transform UEDGE’s core boundary condition from specified density and temperature to specified particle flux and power using the values obtained in the baseline calculation from Sec. 2. These are held fixed during the scan as are all of the transport coefficients (the effects of lithium on SOL transport have not been established). The lower limit of the scan, $\mathcal{R} = 0.65$, is set by the ability of UEDGE to obtain a converged solution. However, the global recycling coefficient (ratio of ion current out through the separatrix to recycled neutral current flowing in) [13], 0.46 at this point, is less than \mathcal{R} .

In Fig. 4a, we show the variation of the core and maximum outer divertor n_e with \mathcal{R} . The former is of interest in planning the LLD experiments and can be compared with the simple particle balance calculations used in establishing the LLD radius and width. The peak divertor n_e and T_e [Fig. 4b] will impact the transport of lithium evaporated or sputtered from the LLD surface. The drop in peak heat flux in going from $\mathcal{R} = 0.95$ to 0.9 is the result of increased power flow to the inner divertor in the latter case. This in turn is associated with a reduction in the electron density peak in the inner divertor at the base of the center stack due to the drop in upstream density. For $\mathcal{R} < 0.85$, this density peak is gone entirely, and further reductions in \mathcal{R} uniformly increase the power load to the outer divertor.

The total recycled gas current flowing away from the outer divertor target [Fig. 4a] drops roughly a factor of 40 over this range of recycling coefficients; the peak D_α emission rate decreases by a similar factor (60). In contrast, the liquid lithium tray experiments on CDX-U yielded D_α emission rates only about a factor of three lower than that obtained with a bare, stainless steel tray [14]. This disparity

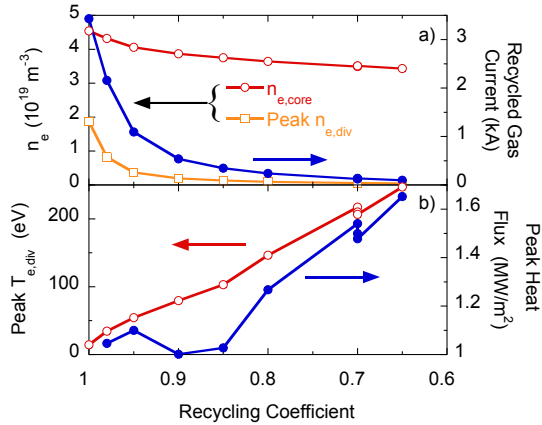


Fig. 4 **a** LLD temperature rise computed with the $\mathcal{R} = 0.65$ heat flux profile. **b** Pulse length required to reach $\Delta T = 200$ °C for a range of \mathcal{R} values.

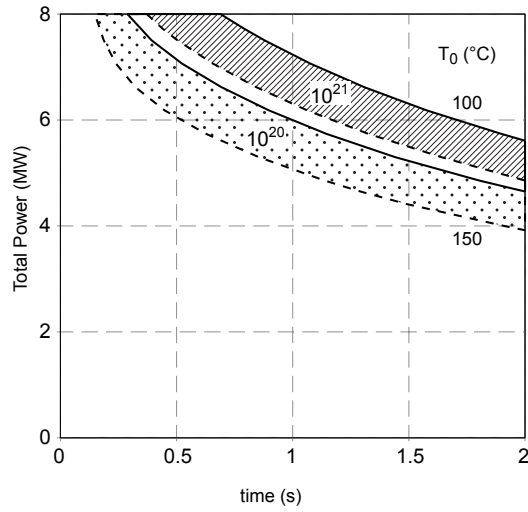


Fig. 5 The four curves provide the time at which the liquid lithium reaches a limiting evaporation rate of either 10^{20} (dotted region) or 10^{21} (hatched region) atoms per second for a given total input power. The bottom of each region corresponds to an initial lithium temperature of 150 °C and the top to 100 °C. The input heat flux profile is based upon the $\mathcal{R} = 0.65$ simulation of Sec. 3.

underscores the practical difficulty in preparing and maintaining a lithium surface capable of approaching the theoretical minimum recycling level.

4 Thermal Response Calculation

We now use the outer divertor (LLD) heat flux profiles from the simulations of Sec. 3 in a thermal conduction calculation to map out the operating space of the LLD via 3-D heat transport calculations with the Cbebm code. The LLD is modeled as a 10 mm copper slab with a 0.5 mm layer of stainless steel on top of it and the a 0.4 mm coating of lithium. The molybdenum film between the stainless steel and lithium is too thin to affect the calculations and is ignored. The width of the modeled surface is that of the outer leg of the UEDGE mesh (i.e., about 11 cm); these (axisymmetric) results are for the full toroidal extent of the LLD. We consider initial temperatures (also the fixed temperature at the bottom of the copper) of $T_0 = 100$ and 150 °C to establish the sensitivity of the results to that assumption.

The actual operating limit for the lithium surface will be estimated in subsequent stages of this modeling effort (Sec. 5). For this paper, we set an upper bound on the total rate of lithium evaporation from the surface of 10^{21} atoms per second, corresponding to about 10% of the particle flux from the core plasma. This would also inject electrons into the plasma at a rate comparable to that from the gas puff for the shot modeled in Sec. 2. We also consider 10^{20} atoms per second as a more conservative limit. In going from the lower to the upper limit on the evaporation rate, the maximum temperature of the lithium surface typically increases from about 400 to 500 °C. The principal result of the calculation is then the time at which these evaporation limits are reached.

To determine the variation of this maximum pulse length with input power, we assume that the outer divertor heat flux profiles of Sec. 3 scale linearly with input power [8]. The heat transfer calculation then yields four boundaries in this maximum pulse length vs. power operating space, one for each combination

of the two initial temperatures (100, 150 °C) and evaporation limits (10^{20} , 10^{21} atoms/second). The boundaries obtained with the $\mathcal{R} = 0.65$ simulation from Sec. 3 are shown in Fig. 5. At the highest input powers available to NSTX (4 MW and above), the pulse length would be restricted to less than 2 seconds, especially if the evaporation rate needed to be kept below 10^{20} particles per second or if the initial temperature of the lithium was well above 100 °C. At lower power levels, the restrictions on the pulse length would be those set by volt-second consumption. The pulse length limits are less severe in the higher \mathcal{R} cases since the fraction of the input power deposited on the LLD is lower for them. For example, in the baseline case of Sec. 2, an input power of 6 MW is required to reach the $T_0 = 100$ °C, 10^{20} atoms/second limit at 2 seconds.

A second limit on the pulse length is set by the saturation of the lithium coating. During initial LLD operation, this coating will be applied by the two LiTER evaporators. Assuming saturation at one D per Li, and uniform coverage of the LLD by the LiTERs, pumping one second of the $\mathcal{R} = 0.65$ simulation (261 A) would require 14 seconds of LiTER operation at the maximum rate of 80 mg/min. This is not a severe constraint since the LiTERs are typically operated for minutes at a time between discharges.

5 Discussion

These calculations represent the initial stage of a collaborative effort to self-consistently model the behavior of lithium in LLD operation and to delineate its operational space. Detailed simulations of the emission and transport of LLD lithium are being performed [15], using the UEDGE-supplied SOL plasma and LLD surface temperature profiles described here, via the REDEP code package coupled to TRIM-SP sputtering calculations. These are 3-D, full process, kinetic simulations, with a D, Li, and C containing plasma impinging on a liquid lithium LLD. Initial REDEP results (for the $\mathcal{R} = 0.65$ case) are encouraging, showing moderate (non-runaway) sputtering, low evaporation, and moderate near-surface Li/D concentrations ($< 10\%$), and with about half of the sputtered Li being transported to LLD-adjacent carbon surfaces and thus potentially aiding the D^+ pumping process. In the next phase of the LLD modeling effort, this simulated lithium source will be input to UEDGE so that the lithium SOL transport and core source can be computed. All of these calculations will be described in subsequent publications.

Acknowledgements This work supported by U.S. DOE Contracts DE-AC02-09CH11466, DE-AC05-00OR22725, DE-FG02-04ER54739, and DE-AC52-07NA27344.

References

- [1] M. ONO et al., Nucl. Fusion **40**, 557 (2000).
- [2] H. W. KUGEL et al., Phys. Plasmas **15**, 056118 (2008).
- [3] H. W. KUGEL et al., J. Nucl. Mater. **390–391**, 1000 (2009).
- [4] D. MANSFIELD et al., J. Nucl. Mater. **390–391**, 764 (2009).
- [5] T. D. ROGNLIEN et al., Contrib. Plasma Phys. **34**, 362 (1994).
- [6] A. Y. PIGAROV, S. I. KRASHENINNIKOV, B. LABOMBARD, and T. D. ROGNLIEN, J. Nucl. Mater. **363–365**, 643 (2007).
- [7] J. N. BROOKS, J. P. ALLAIN, T. D. ROGNLIEN, and R. MAINGI, J. Nucl. Mater. **337–339**, 1053 (2005).
- [8] R. MAINGI et al., J. Nucl. Mater. **363–365**, 196 (2007).
- [9] V. A. SOUKHANOVSKII et al., Rev. Sci. Instrum. **74**, 2094 (2003).
- [10] D. P. STOTLER, and C. F. F. KARNEY, Contrib. Plasma Phys. **34**, 392 (1994).
- [11] A. Y. PIGAROV, S. I. KRASHENINNIKOV, and B. LABOMBARD, Contrib. Plasma Phys. **46**, 604 (2006).
- [12] R. MAJESKI et al., Nucl. Fusion **45**, 519 (2005).
- [13] P. C. STANGEBY, The Plasma Boundary of Magnetic Fusion Devices (Institute of Physics Publishing, Philadelphia, 2000).
- [14] R. KAITA et al., Phys. Plasmas **14**, 056111 (2007).
- [15] J. N. BROOKS, J. P. ALLAIN, Purdue University, Personal Communication (2009).